Spindle Disturbances in Human-Hamster Hybrid (A_L) Cells Induced by Mobile Communication Frequency Range Signals

Thorsten Schrader,[1]* Klaus Münter,[1] Thomas Kleine-Ostmann,[1] and Ernst Schmid[2]

[1]*Physikalisch-Technische Bundesanstalt (PTB), Braunschweig, Germany*
[2]*Radiobiological Institute, University of Munich, Munich, Germany*

The production of spindle disturbances in FC2 cells, a human-hamster hybrid (A_L) cell line, by non-ionizing radiation was studied using an electromagnetic field with a field strength of 90 V/m at a frequency of 835 MHz. Due to the given experimental conditions slide flask cultures were exposed at room temperature in a μTEM (transversal electromagnetic field) cell, which allows optimal experimental conditions for small samples of biological material. Numerical calculations suggest that specific absorption rates of up to 60 mW/kg are reached for maximum field exposure. All exposure field parameters—either measured or calculable—are precisely defined and, for the first time, traceable to the standards of the SI system of physical units. Compared with co-incident negative controls, the results of two independently performed experiments suggest that exposure periods of time from 0.5 to 2 h with an electric field strength of 90 V/m are spindle acting agents as predominately indicated by the appearance of spindle disturbances at the ana- and telophase stages (especially lagging and non-disjunction of single chromosomes) of cell divisions. The spindle disturbances do not change the fraction of mitotic cells with increasing exposure time up to 2 h. Due to the applied experimental conditions an influence of temperature as a confounder parameter for spindle disturbances can be excluded. Bioelectromagnetics, 2008.

Key words: EMF; cell line; spindle disturbances; dosimetry; SI units

INTRODUCTION

The rapidly increasing widespread use of cellular mobile communication within the last two decades has led to scientific and popular concerns about the potential human health hazards of chronic exposure to non-ionizing radiation at typical frequencies of GSM mobile phones (900 and 1800 MHz). The question of whether or not these electromagnetic fields (EMFs) may induce genetic effects or lead to a sensitisation of human cells is a current subject of debate. Attention to this issue was considerably increased in recent years by a large number of in vivo and especially in vitro investigations indicating that radiofrequency (RF) radiation may be capable of causing DNA damage [for a review, see e.g., Brusick et al., 1998; Verschaeve and Maes, 1998; Moulder et al., 1999, 2005; Vijayalaxmi and Obe, 2004]. The primary focus of the studies was to evaluate the ability of RF radiation to induce DNA damage in rodents, cultured rodent and human cells as well as freshly collected human lymphocytes using gene mutations, DNA strand breaks, structural chromosome aberrations, micronuclei, sister-chromatid exchanges or cell transformation. The results of these studies are conflicting, although there is a general tendency to believe that these biological effects are rather unlikely because of the very low associated single photon energy of the EMFs in question. Recently, Speit et al. [2007] confirmed this assumption by an independent repetition of experiments published by the European Union (EU)-funded 'REFLEX' project (Risk evaluation of potential environmental hazards from low energy electromagnetic field exposure using sensitive in vitro methods) [2004]. Performing the alkaline comet assay and the micronucleus test, they could not confirm the clearly positive effects of the 'REFLEX' project, although the same cells (human diploid fibroblasts

Grant sponsors: PTB; Ludwig-Maximilian University.

*Correspondence to: Thorsten Schrader, Physikalisch-Technische Bundesanstalt, Department 2.2: High Frequency and Electromagnetic Fields, Bundesallee 100, D-38116 Braunschweig, Germany. E-mail: thorsten.schrader@ptb.de

Received for review 9 October 2007; Final revision received 11 April 2008

DOI 10.1002/bem.20428
Published online in Wiley InterScience (www.interscience.wiley.com).

ES1), the same equipment and the same exposure conditions (1800 MHz; SAR 2 W/kg) were used. An expert review panel [Moulder et al., 2005] concluded that the majority of the in vitro studies reporting a positive effect were flawed due to poor biological design and/or inadequate dosimetry. Therefore, it is essential to perform further investigations under well-defined experimental conditions and scoring criteria to resolve the controversy concerning the possible risks associated with RF radiation in the human body, especially at the cellular level.

Recent results obtained in mammalian cells after exposure to RF radiation have been interpreted as the production of numerical chromosome aberrations [Tice et al., 2002; Mashevich et al., 2003]. Such a mechanism would be different to that induced by ionizing radiation but could be similar to findings observed for aneugenic (aneuploidy-inducing) chemical agents. In a preliminary report on the induction of spindle disturbances in mammalian cells by RF radiation at 835 MHz [Schmid and Schrader, 2007], we could in fact demonstrate that with increasing field strength from 20 to 90 V/m at a constant exposure time of 0.5 h there was an obvious tendency for an increase in the fraction of damaged anaphases and telophases but a less marked increase in the fraction of damaged metaphases. Until now no reasonable explanations are available which may help to elucidate the underlying mechanisms involved in such RF radiation-induced spindle disturbances. Therefore, the aim of the present study was to evaluate in more detail the capacity of RF radiation at a field strength of 90 V/m to act during a narrow time-dependent window of the mitotic cycle, that is, the passage from metaphase to anaphase. A fast and useful test for detecting spindle disturbances in single mammalian cells during their stages of mitosis was applied which has been used in our laboratory during the last 30 years [e.g., Schmid and Bauchinger, 1976; Adler et al., 1993; Sun et al., 2000; Schmid and Schrader, 2007]. Such studies are directed at potential cellular targets which may be modified by aneugenic agents and which may act as the initial cellular process leading to the production of numerical chromosome aberrations.

MATERIALS AND METHODS

Cell Culture

In contrast to our earlier experiments [Schmid and Bauchinger, 1976; Adler et al., 1993; Sun et al., 2000] which were carried out in Chinese hamster fibroblasts (V79), FC2 cells (kindly provided by Dr. E. Severin, University of Münster, Münster, Germany, and originally obtained by Dr. Tom K. Hei, Columbia University Medical Center, New York, NY), an established human-hamster hybrid (A_L) cell line, has been used for the present study. This cell line containing a standard set of Chinese hamster ovary-K1 chromosomes and a single copy of human chromosome 11 has already been used for our preliminary study on detecting spindle disturbances induced by RF radiation [Schmid and Schrader, 2007]. The FC2 cells were grown as monolayer cultures in RPMI-1640 medium, supplemented with 16% fetal calf serum, 100 units of penicillin and 100 μg of streptomycin per ml of culture medium, at 37 °C in a humidified atmosphere containing 5% CO_2 and 95% air.

The FC2 cells used during the exposure are grown as a monolayer in so-called slide flasks (Nunc type 177453, Wiesbaden, Germany) and thus attached to the microscopic slide during experiment and at all times later on. The FC2 cells cannot move either during or after the exposure. Thus, the experimental result can be preserved for a long time after fixation and the result may be validated again later at any time. The fixed position of the FC2 cells is especially important when we discuss the dosimetry. For each experiment a frozen aliquot from the same stock culture of FC2 cells was thawed and seeded as slide cultures with exponentially growing unsynchronized cells into slide flasks at a density of 5×10^4 cells per slide. After an incubation of 72 h at 37 °C, the FC2 cells were re-fed and maintained at 20–22 °C in a portable incubator during a 6 h transport from the Cytogenetics Laboratory in Munich to the PTB in Braunschweig. After arrival, the cultures were incubated at 37 °C in a humidified atmosphere of 5% CO_2 in air. Twenty hours later, the slide flask cultures were exposed to an EMF at a field strength of 90 V/m.

Application of a μTEM Cell for Exposure of Biological Samples to RF Radiation

Experimental setup. For microwave exposure of biological samples a special setup was used [Schmid and Schrader, 2007]. Due to the calculable electric field strength and the TEM wave propagation excited in the μTEM cell, this setup was adopted by the Physikalisch-Technische Bundesanstalt (PTB) as measurement standard equipment for generating the specified electric field strength up to 1 GHz [Crawford, 1974; Münter et al., 1997; Glimm et al., 1997; Schrader et al., 1999; Nikoloski et al., 2005; GUM-Guideline, 1998]. The experimental setup fulfills the recommended minimal requirements for field exposure proposed by Kuster and Schönborn [2000]. However, the methodologies used in this work

are described in detail as this is the first time that traceability to the SI units is obtained for both measured data and numerical results. The setup can be described as follows. Using a signal generator (SML 03, Rohde & Schwarz, Munich, Germany) with 50 Ω output impedance, a signal of adjustable frequency, amplitude and modulation (here: 835 MHz, $E = 90$ V/m, continuous wave signal without modulation, non-intermitted exposure) is generated and amplified to the required power by an amplifier (Amplifier Research 10W1000). The attenuators provide 50 Ω input and output impedance and are arranged in the signal path at the input and output ports of the μTEM cell to improve its voltage standing wave ratio (*VSWR*) towards the output of the amplifier and towards the input of the power meter (NRVS, Rohde & Schwarz). The μTEM cell itself is optimized to provide a very low *VSWR* close to unity. For the ideal case with $VSWR = 1$, the electric and magnetic field components are in phase and maintain their amplitude at a constant level along the test volume inside the μTEM cell. Therefore, standing waves are avoided as much as possible by the chosen setup. However, not only the mechanical dimensions defining the impedance and the *VSWR* limit the operation; the existence of propagating higher-order modes also has to be avoided. Given that both constraints are fulfilled, Equation (1) holds for the calculation of the electrical field strength [Crawford, 1974; Glimm et al., 1997; Münter et al., 1997; GUM-Guideline, 1998; Schrader et al., 1999; Nikoloski et al., 2005] for frequencies between DC and 1 GHz.

The power meter, again with 50 Ω input impedance, measures the forward power at the output of the second attenuator. Provided the transmission loss of the μTEM cell and the attenuation coefficient factor of the well-matched attenuator #2 are known, it is possible to calculate the rms-value of the adjusted empty field strength E in the μTEM cell as follows

$$E = \frac{\sqrt{k_P P_{ind} D^{-1} Z_{L,nom}}}{d} k_{VSWR} k_{TEM} \qquad (1)$$

where P_{ind} is the measured rms RF power, k_p the correction factor obtained from the calibration certificate for the power meter, $D = 0.1$ the linear attenuation coefficient, Z_L the line impedance of nearly 50 Ω, and $d = 0.03425$ m the distance between septum (inner conductor) and outer conductor of the μTEM cell. For $E = 90$ V/m a feed power of nearly 200 mW is needed at the μTEM cell input. The power meter then reads about 20 mW.

The characteristic impedance Z_L of a coaxial line may be chosen as required (here 50 Ω), but it must be maintained along the line to avoid signal reflections. Measured $S_{11}-$ and S_{22} reflection parameters [Crawford, 1974] of the μTEM cell are below −30 dB (<0.1% of the RF power reflected), thus keeping the VSWR caused by residual reflections below 1.065. Up to 1 GHz the resulting variation of E along the μTEM cell is therefore less than 3.5%. The influence of these ''standing waves'' is not easily compensated, therefore the numerical value of the associated correction factor k_{VSWR} in Equation (1) must be set to 1 as the best estimate and has no effect, but its variance is considered in the uncertainty budget. The correction factor k_{TEM} takes into account that E shows a gradient following a line normal to the septum up to the outer conductor. The variation in E was found numerically to be less than 3%, thus k_{TEM} was set to one and its variance is introduced into the uncertainty budget.

The range of electric field strength investigated here was chosen according to the limits given by ICNIRP Guidelines [1998] as ''Reference levels for occupational exposure to time-varying electric and magnetic fields (unperturbed rms values)'' and ''Reference levels for public exposure to time-varying electric and magnetic fields (unperturbed rms values),'' respectively. For the frequency (835 MHz) used in this investigation, ICNIRP limits the electric field strength to 86.7 and 39.7 V/m, respectively. A first measurement survey conducted at PTB shows that the actual electric field strength emitted by cellular phones in the near-field exhibits a range from 15 to 150 V/m.

Numerical simulations. It has been shown, for instance, by the numerical studies of Popovic et al. [1998] and Burkhardt et al. [1996] that the exposure dose depends critically on the exact geometry of the experimental setup including the cell culture container. Hence, we perform a similar calculation to assess the specific absorption rate (SAR) values during our experiment. All numerical simulations were run on CST's [2007] computer program system ''*Microwave Studio*,'' based on the Finite-Integration-Technique-(FIT)-method. A very comprehensive review of the history and background of FIT is given by Marklein [2002]. The FIT-method is based on the theory of Weiland [1977], who developed the idea further from Yee's [1966] solution of Maxwell's equations in time-domain, but using the full set of Maxwell's equations in integral formulation instead of the differential description. Meanwhile, commercial packages are available for both computational methods treating electromagnetic problems and waves in electrodynamics. Within the FIT-method the volume treated is subdivided into small 3D-blocks (voxels) with orthogonal or tetrahedral geometry (meshing). Each voxel is assigned its material properties, being constant within one voxel. The entire

set of voxels formulates the spatial discretization as a grid representation of the problem treated. Two slightly shifted grids (dual grid) allocate the electric field strength E and the magnetic flux density B using all six field components as a vector representation of E and B. The formulation of the FIT-method ensures the transition and continuity of the fields at the material boundaries (from voxel to voxel). The propagation of energy within the grid is computed in a leap-frog scheme, with the time now discretized into small steps. The maximum stable time step can be obtained from the Courant–Friedrichs–Lewy condition [1928], which relates the smallest grid cell size to the wavelength. Very small grid cells (voxels) force very small time steps and long computational time, respectively. The discretization in space and time also introduces numerical errors such as dissipation or dispersion, which cannot all be compensated for.

In the present work we computed the scattering parameters, field strength distribution, and the SAR according to Equation (2) (see below) within the medium of the μTEM cell. For this purpose, the μTEM cell was modeled with a spatial resolution between 0.14 mm and 1.4 mm resulting in 4.9 million voxels for the whole numerical model of the μTEM cell containing the slide flask, the medium and the monolayer of the human-hamster hybrid cells (Fig. 1). For the volume of the medium we have used 225000 voxels (dx, $dy = 0.2$ mm, $dz = 0.49$ mm). To obtain proper scattering parameters the feeding coaxial sections were also discretized with high spatial resolution. The material properties used in the numerical model are the following:

NUNC slide flask with a cover made of polystyrene ($\varepsilon'_R = 2.5$, $\tan\delta = 4 \times 10^{-4}$), the microscope slide is made of soda lime glass ($\varepsilon'_R = 7.75$, $\tan\delta = 9 \times 10^{-3}$). The flasks were always set with their long extending side of the microscope slide (across from twisted cap site) against the septum's transition from a plate to a round center conductor, which is used thereby as a mechanical block while moving the flask towards the feeding port of the μTEM cell.

RPMI-1640 medium ($\varepsilon'_R = 76.2$, $\sigma = 1.45$ S/m, $\rho = 1$ g/ml, measured data).
μTEM cell's septum made of brass ($\sigma_{brass} = 3.0 \times 10^7$ S/m).
μTEM cell's outer shell made of aluminum ($\sigma_{alu} = 4.0 \times 10^7$ S/m).

Estimation of the SAR values. Calculating the specific absorption rate SAR as given in Equation (2), with the electrical field strength E_{media} inside the medium, the conductivity σ and the density ρ of the medium, the dosimetry can be estimated and used for comparison with other experimental setups.

$$SAR = \frac{1}{2}\frac{\sigma |E_{media}|^2}{\rho} \qquad (2)$$

It shall be mentioned here for the sake of clarity, that the (empty) field strength E in Equation (1) and E_{media} in Equation (2), respectively, may differ significantly depending on the dielectric properties of the medium.

Due to the accumulation of the FC2 cells in a thin monolayer directly on top of the microscope slide, we computed the SAR distribution in an appropriate test volume. In Figure 2, the numerically computed SAR distribution 0.1 mm above the microscope slide is shown for 200 mW rms feed power. The rectangle in Figure 2 indicates the area in which the monolayer of the FC2 cells is evaluated. The SAR value ranges from 10.7 to 17.2 mW/kg at the location of the evaluated FC2 cells. Additionally, Figure 3 shows the SAR distribution in the cross-section, indicating that the SAR value directly above the microscope slide is significantly lower compared to the rest of the liquid. In the unloaded lower half of the μTEM cell the empty field strength was numerically calculated to 95.5 V/m. This value is in good accordance (deviation less than 3.5%) with the exact value of 92.3 V/m, which can be predicted for an empty μTEM cell by Equation (1) with $P = 200$ mW and a septum separation of $d = 0.03425$ m. This

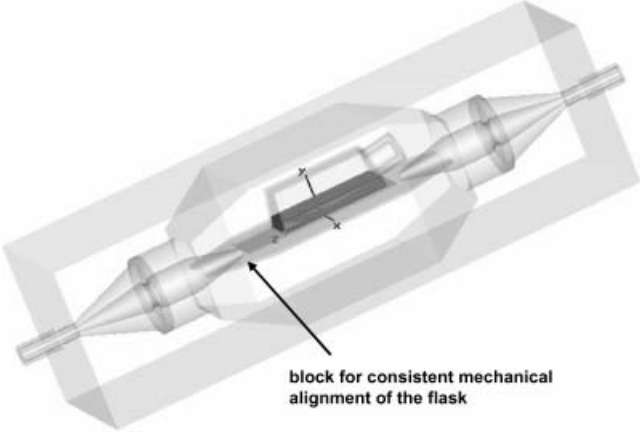

Fig. 1. Close-up view of the numerical model of the NUNC slide flask type 177453 filled with RPMI-1640 medium ($\varepsilon'_R = 76.2$, $\sigma = 1.45$ S/m measured data) set on the septum of the μTEM cell. The cover is made of polystyrene ($\varepsilon'_R = 2.5$, $\tan\delta = 4 \times 10^{-4}$), the microscope slide is made of soda lime glass ($\varepsilon'_R = 7.75$, $\tan\delta = 9 \times 10^{-3}$). The flasks were always set with their long extending side of the microscope slide (across from twisted cap site) against the septum's transition from a plate to a round center conductor, which is used thereby as a mechanical block while moving the flask towards the feeding port of the μTEM cell.

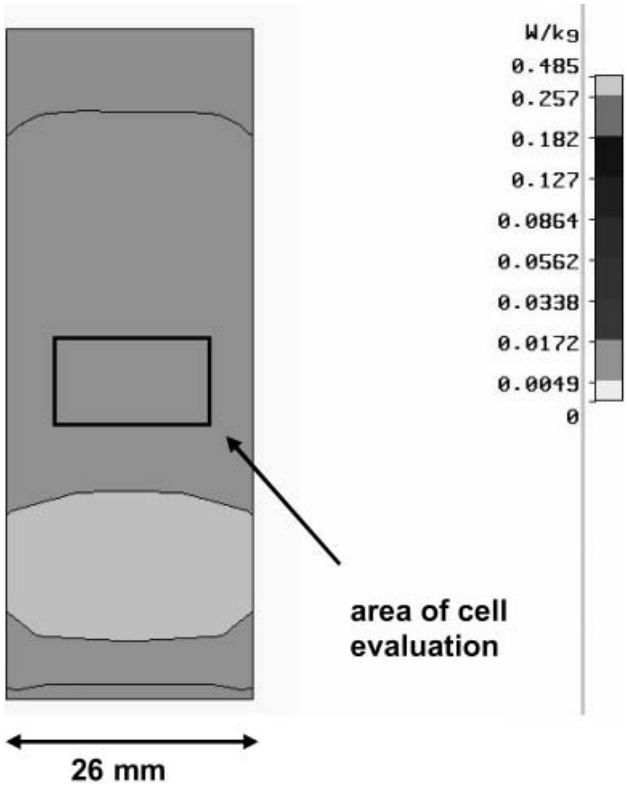

Fig. 2. *SAR* distribution in the medium in 0.1 mm height above the microscope slide carrying the monolayer of the human-hamster hybrid cells computed at 835 MHz. The rectangle indicates the area in which the monolayer was evaluated to avoid any influence from an inhomogeneous SAR distribution.

comparison of the empty field strength established according to Equation (1) with the value obtained from numerical computation provides the link needed between the experimental setup and the numerical model.

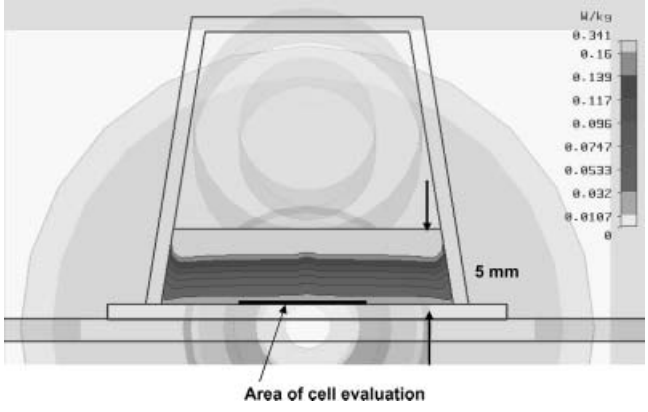

Fig. 3. Cross-section of the fluid indicating the local *SAR* distribution at 835 MHz in transverse direction, indicating a maximum *SAR* value of 62.5 mW/kg in the area of the monolayer. The bar shows the area of FC2 cells evaluated.

Considering the loaded upper half of the μTEM cell, the resulting field strength inside the medium 0.1 mm above the glass slide was calculated to 3.98 V/m using infinitely small virtual field probes to obtain the resultant field strength in the media from the numerical calculations. With Equation (2) and the given material parameters the corresponding SAR can be calculated to be 11.5 mW/kg. The SAR distribution in the whole cell medium is clearly non-uniform due to the different dielectric properties at the adjacent medium-air and medium-glass boundaries, respectively. However, as we are interested in the SAR value in a very restricted test volume out of the 5 ml fluid, the average was calculated for 0.001 g. Still, the average cell weight with 2.12×10^{-5} g is almost 2 orders of magnitude below the average value. These data are valid for all SAR values indicated in this work.

Using a fixed monolayer of FC2 cells we gain several advantages. First, the non-uniform SAR distribution due to the edge effects does not impact the test volume, if severe heating is avoided. Then the surrounding medium causes the *E*-field distribution (and SAR) to be homogeneous in the embedded test volume. This was not considered in other experiments [Nikoloski et al., 2005], where the cells were able to float inside the media. Within the same experiment [Nikoloski et al., 2005] the local SAR distribution varied by 15 dB (a linear factor of 31.6 in terms of power). In the present experiment, we have reduced the variation to 1.64 (linear) or 2.1 dB in terms of power, respectively.

In our experiment the uncertainty of the SAR during exposure is dominated by the uncertainty of the E-field representation. The measurement uncertainty of *E* can be obtained using Equation (1). This procedure is in accordance with the ''Guide to the Expression of Uncertainty in Measurement'' [GUM-Guideline, 1998] and those procedures used by the National Metrology Institutes, when they compare their capabilities of measurement and calibration in international round robin tests. For the coverage factor $k = 2$, the expanded measurement uncertainty *U* of the (empty) electric field strength is estimated to be 10%. The uncertainty of the SAR value in the numerical computation depends on the uncertainty of the material parameters and on the spatial resolution and details of the model.

Influence of thermal aspects. To be able to exclude thermal effects, we have to estimate the temperature increase of the sample during the field exposure. An upper limit of the deposited power and the heating induced thereby can be derived from the scattering parameters of the μTEM cell. These are traceable to the SI units, if measured with a vector network analyzer (VNA). The forward (S_{21}) and reverse (S_{12}) transfer

scattering parameters indicate any RF power losses inside the μTEM cell. The empty μTEM cell is a special case of a reciprocal twoport, where S_{21} exactly equals S_{12}. Therefore, the arithmetic mean of both $(|S_{21}| + |S_{12}|)/2$ is taken as the best estimate for the transfer parameter. Measured results for the μTEM cell are presented in Figure 4. The power transmission parameter $[(|S_{21}| + |S_{12}|)/2]^2$ of the unloaded (empty) cell was very near to one over the complete frequency range, clearly indicating that the cell alone is nearly perfectly lossless. As expected, this did not change much when the slide flask was inserted, first empty and then filled with 5 ml of medium. Filling the slide flask did not make a significant difference since the liquid forms only a thin layer in the slide flask. Over the frequency range of the GSM (''D'') band the transfer parameters stay well above 0.99 both for the empty μTEM cell and for the μTEM cell loaded with the empty slide flask, implying that a maximum fraction of 0.01 ± 0.002 ($1 \pm 0.2\%$) of the μTEM cell input power is dissipated or reflected somewhere on its way, excluding any relevant temperature increase of the μTEM cell. At 835 MHz the power transfer parameter $[(|S_{21}| + |S_{12}|)/2]^2$ decreases by 0.0023 ± 0.002 ($0.23 \pm 0.2\%$) when the slide flask is filled with medium. Since the measurement value is in the order of the uncertainty we can only derive an upper limit, but not an exact value of the SAR. The maximum μTEM cell input power applied during the field exposure of the samples was 200 mW, and accordingly the dissipated power should always be below (0.46 ± 0.4) mW. This power is mostly absorbed in the 5 ml (≈ 5 g) of fluid culture medium, resulting in an estimated average SAR value of (92 ± 80) mW/kg and, hence, in an upper limit of 172 mW/kg. However, the simulation suggests that at 200 mW power incident into the μTEM cell, *SAR* values of 111.1 mW/kg (calculated for the whole medium and thus, significantly larger than in the monolayer) can be expected, which is within the range given by the scattering parameter measurements.

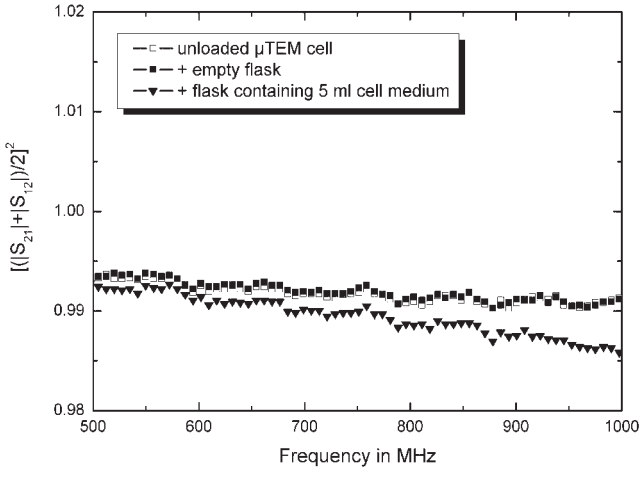

Fig. 4. Power transmission factor calculated from the arithmetic mean of linear transmission scattering parameters $[(|S_{21}|+|S_{12}|)/2]^2$ of the μTEM cell with and without loading.

The bottom area (10 cm^2) of the slide flask was always in good thermal contact (Fig. 1) with the μTEM cell's septum at ambient temperature (thermal conductivity of soda lime glass of 1.1 W/mK). For the given bottom area and a dissipated power of 0.46 mW we obtain 0.046 mW/cm^2 conducted into the metal septum surface. Thus, we expect a balance between the input power and the dissipated heat of the sample. This was experimentally verified by continuous online measurements using the fiber optical thermometer Fotemp4 (Optocon, Dresden, Germany) and the probe TK5/2 (0.55 mm thickness) with proven biological compatibility. This probe is nearly without impact on the field distribution during exposure as it is metal-free and consists only of a fiber-coupled semiconductor probe tip. Two hours exposure at 90 V/m produced a temperature rise of less than 0.15 K, therefore it was repeated with 500 V/m. The temperature increase of the liquid was then 0.8 K, corresponding to a heat dissipation of 12.17 mW within 5 g of liquid (SAR of 2.43 W/kg). At 90 V/m this gives a SAR value of 79 mW/kg which is consistent with the previous estimates.

In Vitro Assay for Spindle Disturbances

Exposure to RF radiation. Slide flask cultures of FC2 cells were exposed at room temperature (20–22 °C) to an EMF at a field strength of 90 V/m applying time periods up to 2 h. Immediately after exposure, the FC2 cells were fixed on the slides according to our standard procedure for this assay for spindle disturbances [Schmid and Bauchinger, 1976; Adler et al., 1993; Sun et al., 2000], that is, for fixation one third of the medium was replaced by a mixture of three parts of 99% ethanol and one part of glacial acetic acid. The fixation procedure was repeated three times over a period of 15 min. By using this method the cytoplasm of the cells remained well-preserved and chromosome loss due to preparational procedures was avoided. All slides were coded. After air-drying the cells were stained with 2% acetic orcein (Gurr, Wycombe, UK). Due to the given experimental conditions at the laboratories in Munich and at the PTB, 9876 FC2 cells were analysed for controls which were kept unexposed either at 37 °C or parallel with the RF radiation exposures at room temperature of 20–22 °C. The fraction of mitotic cells was determined by scoring 3000 cells per slide.

Exposure to trichlorfon (positive control). The insecticide trichlorfon which can induce spindle disturbances in V 79 cells and aneuploidy in male mouse germ cells, especially by affecting the chromosome segregation [Sun et al., 2000] was tested as the positive control for demonstrating the adequacy of the experimental conditions to detect a known spindle acting agent. To compare the sensitivity of the current test system (based on FC2 cells) with that of our earlier test system (based on V79 cells), the experimental schedule for detection of spindle disturbances in V79 cells by trichlorfon was only modified by using FC2 cells. Since cell preparation, culture technique and fixation procedure have been reported in detail earlier [Schmid and Bauchinger, 1976; Adler et al., 1993; Sun et al., 2000], only a brief description is given here. Slide cultures (2×10^5 FC2 cells/slide) were set up in slide flasks and incubated at 37 °C. After 24 h the cells were fed with medium containing 100 μg/ml trichlorfon dissolved in aqua bidest for exposure periods up to 6 h at room temperature (20–22 °C). Immediately after exposure, the cells were fixed and stained in the same way as described for exposure to RF radiation.

Scoring criteria for spindle disturbances. Mitoses with spindle disturbances at metaphases or at ana- and telophases were distinguished. Partial or complete disturbance of the spindle apparatus was indicated by the appearance of (a) initial c-metaphases [Schmid and Bauchinger, 1976] where chromosomes were not distributed over the entire cell area, but were arranged in several groups (multiple-group metaphases) or concentrated in the center of the cell (the appearance of ball metaphases resulting from monopolar spindles), (b) typical c-metaphases (contracted chromosomes completely scattered in the cytoplasm, characteristic of colchicine-treated cells), and (c) improper alignment of single chromosomes onto the metaphase plate (non-congression). Spindle disturbances of ana- and telophase figures particularly exhibit configurations with lagging or non-disjunction and multipolar distribution of individual chromosomes. The appearance of ana- and telophases with bridges and/or breaks can be considered as indicators of clastogenic activity, that is, the induction of structural chromosome aberrations.

Statistics

A null hypothesis, that the proportions of FC2 cells with spindle disturbances in the two independently performed experiments are not different, was tested according to the method of Kazmier and Pohl [1987]. For each exposure level, the two sample proportions (one from each experiment) were pooled for the purpose of determining both the standard error of the difference between proportions and the pooled estimate of the population proportions. Since the conditions for the applications of the normal probability distribution hold for these data (i.e., both sample sizes are much larger than 100 cells and the products of sample sizes and proportions are greater than five), the observed difference between the two sample proportions could be converted into the z-test statistics. A difference at the two-sided P-value <0.05 was considered statistically significant.

RESULTS

The influence of the electric field strength of 90 V/m on FC2 cells was investigated applying exposure periods up to 2 h. The result of the mitotic figure analyses is presented in Table 1, together with coincident negative control data. The frequency of mitoses (%) with normal and damaged mitotic figures in cells was determined in two independently performed experiments to demonstrate reproducibility and indicate inter-test variability. No significant differences between the first and replicate experiment (8 weeks later) of the most frequent damage, that is, ana- and telophases with spindle disturbances, have been observed. It is demonstrated in Table 2, that none of the resulting two-sided P-values were less than 0.2, so the null hypothesis could not be rejected at either the 5% or the 10% levels of uncertainty. It is evident that an electric field strength of 90 V/m can impair a normal formation or function of the mitotic spindle (Table 1). In Figure 5, a normal metaphase (a) and a normal late anaphase (b) is shown. Mitoses with clearly analysable distribution defects were found either at the metaphase or the ana- and telophase stage of cell divisions. Within the exposure time from 0.17 to 2.0 h the total frequencies of mitoses with spindle disturbances were always more than four times higher than the corresponding control value. Abnormal metaphases, predominately with non-congression (Fig. 5c) or initial c-metaphases, comprised less than about 40% of the total spindle disturbances. About 60% of the total spindle disturbances were ana- and telophase figures particularly exhibiting configurations with lagging or non-disjunction (Fig. 5d–f). For both experiments, the fraction of ana- and telophases with spindle disturbances versus the exposure time to the EMF is shown in Figure 6. It increases with increasing exposure time from a low spontaneous fraction to a saturation value of about 20%. The lower fraction determined for 0.17 h exposure appears to reflect the time period for reaching an equilibrium of ana- and telophases, during time interval formation exceeds loss or gain by cell division turnover. The frequency of ana- and telophase figures

TABLE 1. Frequency of Mitoses (%) With Normal and Damaged Mitotic Figures Observed in Human-Hamster Hybrid Cells After Exposure to an Electric Field Strength of 90 V/m for Varying Periods of Time

	1. Experiment					2. Experiment				
Exposure time (h)	0	0.17	0.5	1	2	0	0.17	0.5	1	2
Cells analyzed	1000	1050	1080	1030	1336	1548	2102	2003	2114	2631
Normal mitotic cells	99.0	95.0	95.2	93.0	90.3	99.5	95.0	95.4	93.9	92.6
Prophases	12.9	15.3	14.0	17.1	14.2	11.0	15.7	20.0	19.9	11.0
Metaphases	69.2	64.7	68.2	63.2	49.8	66.0	64.3	63.5	64.4	61.9
Ana-telophases	16.9	15.0	13.0	12.7	26.3	22.5	15.0	11.9	9.6	19.7
Mitoses with spindle disturbances	0.90	4.48	4.44	6.70	8.76	0.32	4.61	4.49	5.82	7.15
Metaphases with initial c-mitosis	0.40	0.48	0.37	1.94	0.97	0	0.38	0.30	2.18	0.49
c-mitosis	0.10	0.19	0.19	0.10	0.52	0.06	0.24	0.50	0.24	0.38
Non-congression	0.10	1.43	1.02	1.36	1.12	0	1.28	0.60	0.90	0.87
Ana-telophases with multipolar distribution	0.10	0.57	0.28	0.49	0.45	0	0.52	0.40	0.33	1.14
Lagging	0.20	0.95	1.48	0.97	1.12	0.13	0.95	1.00	0.66	1.03
Non-disjunction	0	0.86	1.11	1.84	4.57	0.13	1.24	1.70	1.51	3.15
Ana-telophases with bridges and/or breaks	0.10	0.48	0.37	0.30	1.05	0.19	0.43	0.10	0.28	0.26
Mitotic index (% ± SD)	2.67 ± 0.30	2.73 ± 0.30	2.23 ± 0.27	2.57 ± 0.29	1.83 ± 0.25	2.53 ± 0.29	2.90 ± 0.31	2.43 ± 0.28	2.73 ± 0.30	2.00 ± 0.26

with bridges and/or breaks (fragments of chromosomes) was not significantly increased.

To test the sensitivity of FC2 cells for detecting potential spindle disturbances, our earlier experiment with a 6 h exposure period of V79 cells to the aneugen trichlorfon [Sun et al., 2000] was repeated in FC2 cells applying exposure periods up to 6 h. Table 3 shows that the frequency of mitosis with spindle disturbances (24.0) induced by a 6 h exposure to trichlorfon in FC2 cells was only about 70% of that (33.1) obtained earlier in V79 cells under similar experimental conditions, although the aberration pattern in both cell lines remained unchanged. Figure 7 shows that the fraction of ana- and telophases with spindle disturbances versus the exposure time of RF-EMF radiation up to 2 h (pooled data of two independent experiments, Table 1) is very different to the corresponding data of trichlorfon (Table 3) indicating different mechanisms of origin for producing spindle disturbances.

To examine any influence of the incubation temperature (37 °C) or the exposure temperature (20–22 °C) on the frequency of cells with spindle disturbances, several negative control experiments were analysed. The frequencies of mitoses (%) with normal and damaged mitotic figures observed in the FC2 cells without any exposure to an electric field strength are summarized in Table 4. There is no evidence of inhomogeneity in the control data subdivided into four groups according to their cell culture temperatures including the pooled data of the coincident negative controls of RF-EMF radiation exposures (Table 1). None of the frequencies of the damaged cells from the separate control samples are more than 1.5 standard deviations away from the Poisson means that were obtained from scaling the mean of the pooled data to the four individual sample sizes. Therefore, the given experimental conditions at the PTB had no subtle effect on evaluating the predicted spindle-acting capacity of the EMFs in question in FC2 cells. As generally observed, only the frequency of mitotic cells (%) is lower at room temperature (2.60 ± 0.30) than that at incubation temperature (3.93 ± 0.36).

DISCUSSION

The present study suggests that an electric field strength of 90 V/m is a spindle acting agent in human-hamster hybrid cells as indicated by the appearance of spindle disturbances at the metaphase stage (especially non-congression configuration) and preferably at the ana- and telophase stages (especially lagging and non-disjunction of single chromosomes) of cell divisions. Unlike the induction of DNA alterations, where the

TABLE 2. The *z*-Test Statistics for the Difference of Proportions of Ana- and Telophases With Spindle Disturbances Between Fraction F1 (First Experiment) and Fraction F2 (Replicate Experiment) at Each Exposure Level

Duration of exposure (h)	Fraction F1 (±SE) of ana-telophases with spindle disturbances	Fraction F2 (±SE) of ana-telophases with spindle disturbances	*z*-value	Two-sided *P*-value
0	0.0173 ± 0.01	0.0113 ± 0.0056	0.52	>0.5
0.17	0.133 ± 0.0266	0.1496 ± 0.0198	−0.50	>0.5
0.5	0.1771 ± 0.0318	0.2053 ± 0.0261	−0.69	0.45
1	0.2024 ± 0.0347	0.2023 ± 0.0278	0.00	>0.5
2	0.1835 ± 0.0203	0.2105 ± 0.0178	−1.00	0.27

Significance is considered at two-sided *P*-values less than 0.05

target is clearly defined, spindle disturbances may result from damage to the functioning of a variety of cellular targets. These include targets common to mitotic cell division such as highly dynamic microtubules, microtubule-based motors, microtubule-associated proteins, and condensed chromosomes as important structural components of the spindle morphogenesis. The very complex protein superstructure of the spindle [for a review, see e.g., Compton, 2000] is based on a bipolar array of microtubules, each of which is a polarised protein polymer with a plus and a minus end. It is known that any defects in spindle bipolarity lead to potential errors in chromosome segregation and that microtubule attachment to the kinetochores can be disrupted by chemical agents, chromosome micromanipulation or antibodies to centromere proteins [for a review, see e.g., Inoue and Salmon, 1995]. Missegregation of chromosomes during mitosis can cause numerical chromosome aberrations giving rise to aneuploidy in daughter cells which can lead to severe adverse effects in humans, for example, it may be associated with carcinogenesis [Duesberg et al., 2000]. There are two processes which may act as the initial cellular insult leading to aneuploidy in daughter cells, one is non-disjunction and the other is chromosome loss. Chromosome loss means that chromosomes are not included in the main nuclei and become micronuclei [Parry et al., 1995], while non-disjunction means that a chromosome pair goes to one nucleus only resulting from malfunction of one of many processes involved in faithful segregation of chromosomes during mitosis [for a review, see e.g., Vig, 1993].

Non-disjunctions of single chromosomes were the most frequent spindle disturbances at the ana-

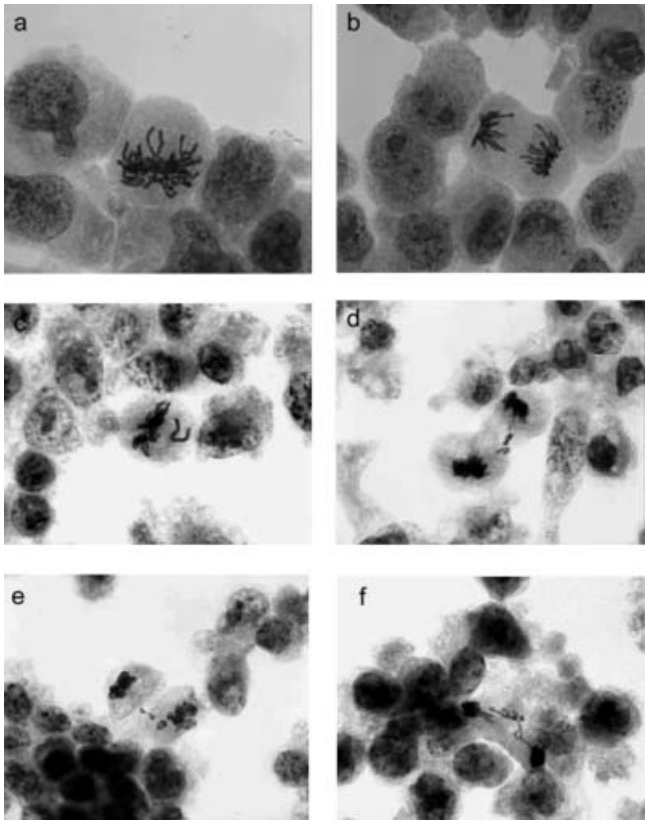

Fig. 5. Metaphases and ana- or telophases of FC2 cells: (**a**) normal metaphase; (**b**) normal late anaphase; (**c**) metaphase with non-congression; (**d**–**f**) ana- and telophases with non-disjunction or lagging chromosomes.

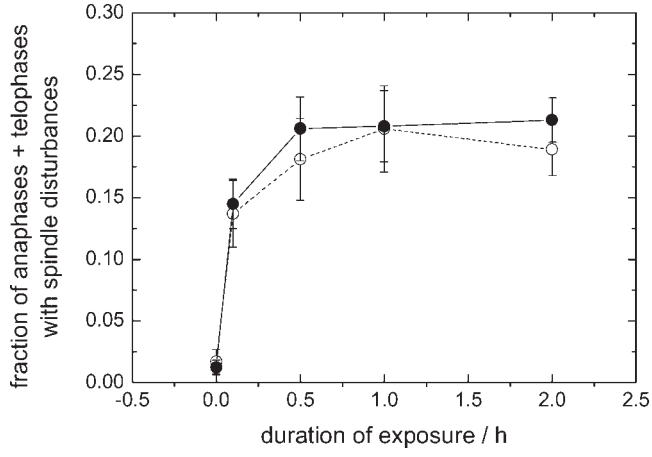

Fig. 6. Fraction of ana- and telophases with spindle disturbances in FC2 cells in its dependence on the duration of the EMF exposure time at 90 V/m. Results of two independently performed experiments. Each point is based on >1000 analyzed cells. Standard errors (SE) are indicated by vertical bars.

TABLE 3. Frequency of Mitosis (%) With Normal and Damaged Mitotic Figures After Exposure to Trichlorfon (Positive Control) Observed in FC2 Cells as well as in V79 Cells of an Earlier Study [Sun et al., 2000]

	FC2 cells					
Exposure time (h)	0	0.17	0.5	2	6	V79 cells 6
100 µg/ml trichlorfon						
Cells analyzed	1000	1047	1114	1161	1000	1000
Normal mitotic cells	99.1	98.7	98.8	92.7	75.7	64.3
Prophases	13.8	12.2	11.9	10.4	13.7	15.3
Metaphases	68.9	52.1	56.6	48.3	42.5	38.5
Ana-telophases	16.4	34.4	30.3	34.0	19.5	10.5
Mitoses with spindle disturbances	0.80	1.15	1.08	6.97	24.0	33.1
Metaphases with						
Initial c-mitosis	0.20	0.29	0.27	1.72	4.80	7.1
c-mitosis	0.20	0.19	0.27	2.41	14.20	20.7
Non-congression	0	0.10	0.18	0.52	3.30	5.3
Ana-telophases with						
Multipolar distribution	0	0.19	0.09	0.43	0.30	0.3
Lagging	0.30	0.19	0.09	0.86	0.70	0.8
Non-disjunction	0.10	0.19	0.18	1.03	0.70	0.2
Ana-telophases with bridges and/or breaks	0.10	0.19	0.09	0.33	0.30	0.6
Mitotic index (% ± SD)	4.37 ± 0.38	3.13 ± 0.32	2.93 ± 0.31	3.00 ± 0.32	3.50 ± 0.34	2.30 ± 0.28

and telophases observed in the present experiments (Table 1). However, it remains to be clarified why RF radiation can disturb spindle function in these human-hamster hybrid cells. Therefore, additional considerations are required that are related to the choice of biological damage indicators as well as their cell cycle kinetics. Many of the earlier studies assayed cellular damage indicators which had been shown to be typically associated with ionizing radiation. Therefore, comprehensive investigations of the potential clastogenicity of mobile communication frequency range were predominately performed in human lymphocytes during the DNA pre-synthetic (G_0 phase) of the cell cycle. While there was no indication of any induced chromosome changes in most of these studies [Moulder et al., 1999; Stronati et al., 2006; Scarfi et al., 2006], Tice et al. [2002], for example, reported a significant increase of micronuclei in unstimulated human lymphocytes for a 24 h exposure to EMF (837 MHz) at SAR values of 5 and 10 W/kg, whereas a 3 h exposure did not induce this biological effect. Since the authors could not observe any increase in DNA damage (strand breaks/alkali labile sites) under the same exposure conditions, they speculated that numerical chromosome aberrations may be involved in the positive findings. Such an assumption is based on the fact that micronuclei may not be derived solely from chromosome fragments which have failed to become incorporated into the macronuclei of daughter cells at anaphase (structural aberrations). Micronuclei can also be formed by the loss of whole chromosomes at mitosis (numerical aberrations) and exist separately from the main nucleus of a cell. Although several excellent methods are available to identify the presence of centromeres or centromere-associated structures within the micronuclei (e.g., staining techniques with kinetochore antibodies or DNA probes), the possibility of analysing the two major mechanisms of origin was not employed. Using a more suitable cytogenetic assay for investigating a suspected aneugen, Mashevich et al. [2003] reported that a 72 h exposure of PHA-stimulated human lymphocytes to continuous 830 MHz EMFs in fact caused a SAR dependent aneuploidy. At SARs from 1.6 to 8.8 W/kg, losses and gains of chromosome 17 were determined by applying a fluorescence in situ hybridisation (FISH)

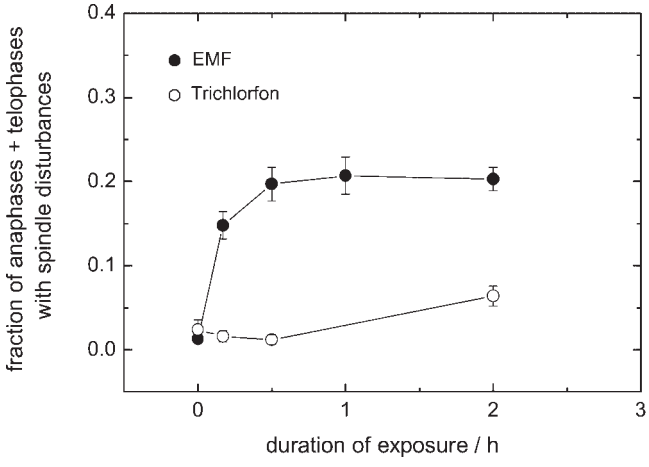

Fig. 7. Fraction of ana- and telophases with spindle disturbances in FC2 cells induced by the EMF as well as the positive control trichlorfon in its dependence on the duration exposure time. Each point is based on >1000 analyzed cells. Standard errors (SE) are indicated by vertical bars.

TABLE 4. Frequency of Mitoses (%) With Normal and Damaged Mitotic Figures Observed in Human-Hamster Hybrid Cells Without Any Exposure to an Electric Field Strength

Timing of control analysis	Before departure from GSF	After arrival at PTB	After 20 h incubation at PTB	Parallel with EMF exposure at PTB
Culture temperature	37 °C	22 °C	37 °C	22 °C
Cells analyzed	3140	2280	1908	2548
Normal mitotic cells	98.9	99.3	98.7	99.3
Prophases	13.8	16.0	10.7	11.7
Metaphases	68.9	68.4	67.8	67.3
Ana-telophases	16.2	14.9	20.3	20.3
Mitoses with spindle disturbances	0.96	0.61	1.05	0.55
Metaphases with				
Initial c-mitosis	0.32	0.18	0.31	0.16
c-mitosis	0.24	0	0.05	0.08
Non-congression	0.10	0.09	0.10	0.04
Ana-telophases with				
Multipolar distribution	0.06	0	0.05	0.04
Lagging	0.22	0.26	0.26	0.16
Non-disjunction	0.03	0.09	0.31	0.08
Ana-telophases with bridges and/or breaks	0.10	0.09	0.21	0.16
Mitotic index (% ± SD)	4.27 ± 0.38	2.23 ± 0.27	3.93 ± 0.36	2.60 ± 0.30

technique using a directly labeled commercial probe for the centromeric repetitive DNA arrays.

Our present results confirm in essence the findings of Mashevich et al. [2003] and—with some restrictions—the results of Tice et al. [2002], that RF radiation may induce numerical chromosome aberrations in proliferating cells. Therefore it can be suggested that the arguments associated with both former experiments were essentially valid and, specifically, that it was an adequate approximation to refer the effect of RF radiation to functional disturbances of the spindle apparatus but not to structural alterations of DNA. It can be assumed that proteins which regulate the pathway of chromosome segregation during mitosis may be altered by EMFs. Such an assumption would explain the former observations that induction of spindle disturbances in human lymphocytes appears to depend on whether or not the lymphocytes were PHA-stimulated before RF radiation exposure. The same argument may also be valid for the recent findings of Vijayalaxmi [2006], who could not observe any elevated yields of micronuclei in human lymphocytes. Since the PHA-stimulation was only 24 h before the in vitro exposure to 2.45 or 8.2 GHz RF radiation, it can be assumed that RF radiation could not directly act on mitotic figures at this early culture time. The results of the present experiment for a field strength of 90 V/m at an exposure time of 0.5 h (Table 1), that is, about half of a mitosis cycle, indicate a direct effect on the spindle apparatus during metaphase or ana- and telophase. The lower fractions of ana- and telophases with spindle disturbances determined for 0.17 h exposure to EMF (Fig. 6) appear to reflect the time period for reaching an equilibrium of ana- and telophases, during time interval formation exceeds loss or gain by cell division turnover. These findings seem to suggest that the micronuclei formed by EMF-induced loss of whole chromosomes at mitosis should be essentially produced during time period of polymerisation or depolymerisation of microtubule. From an experimental point of view, it is not surprising that the present results of elevated fractions of mitoses with spindle disturbances after EMF exposure differ from those obtained in studies using micronuclei as biological endpoints. The reason is that micronuclei were scored after EMF- or chemical agent exposure—in accordance with standard procedures—in cells cultured for at least one more cell division in the presence of cytochalasin B. Therefore, many cells which were not exposed to EMF could also reach the binucleated stage of cell division, thus showing decreased yields of micronuclei.

In view of these somewhat complex considerations, it is not surprising that our results obtained for the positive control are not directly comparable with those of EMF exposure. Trichlorfon as a chemical aneugen needs an exposure period longer than 2 h to induce spindle disturbances (Table 3, Fig. 7). Therefore, the EMF-induced effects are rather unusual for an aneugenic mode of action, because of the immediate effects after exposure for a short period of time. It can be concluded that different underlying mechanisms

for the production of spindle disturbances by EMF or aneugenic chemicals are responsible. Thus, it is not surprising that in contrast to the spindle-damaging property of EMF, in our earlier studies on detecting aneugenic chemicals [Schmid and Bauchinger, 1976; Adler et al., 1993; Sun et al., 2000] an onset of a metaphase block was indicated by a markedly elevated number of cells arrested at metaphase and a simultaneously reduced number of cells entering ana- and telophase resulting in a concentration-dependent increase of the fraction of mitotic cells. Although a number of mechanisms are known by which chemicals might increase the incidence of chromosome segregational errors [Oshimura and Barrett, 1986], until now none can explain the observed spindle-disturbing potential of EMF.

An important source of misinterpretation of findings indicating an induction of spindle disturbances in mammalian cells by EMF is certainly the fact that such biological effects can also be produced via thermal pathways. For example, Vijayalaxmi and Obe [2004] argued as a plausible explanation for the significant increase of micronuclei after a 24 h exposure of unstimulated human lymphocytes to EMF observed by Tice et al. [2002], that ''the observed effects could be due to a highly localized increase in temperature.'' This argument may be plausible, because it has been well-known for seventy years that hyperthermia can induce aneuploidy in plants [Sax, 1937]. In fact, it is a highly debated question whether or not several biological effects which have been observed after EMF exposure of different samples should be attributed to an elevation in the sample temperature, or whether they may be due to RF radiation itself. However, it should be taken into account that, compared with the extensive investigation of a temperature-dependent induction of structural chromosome aberrations by ionizing radiation (especially using hyperthermia, >39 °C) [Vijayalaxmi and Obe, 2004], relatively little information has been published on numerical chromosome aberrations produced via thermal pathways. After exposure of PHA-stimulated human lymphocytes to a temperature of 43 °C for 1 h, significantly elevated levels of aneuploid cells, with both losses and gains of chromosomes at the metaphase stage of the cell division, could be observed [Prabhakara and Murthy, 1995]. This result could be confirmed by Mashevich et al. [2003] in experiments without any RF radiation on PHA-stimulated human lymphocytes. Using FISH painting technique for chromosome 17, they found a significant increase in the aneuploidy level at temperatures of 40–41 °C, but no indication for any influence on the aneuploidy level at lower temperatures from 34.5 to 38.5 °C. In our study such an influence via thermal pathways (hyperthermia) can be ruled out because the slide flask cultures were exposed to NIR, not only at far lower temperatures (20–22 °C), but also under experimental conditions where the temperature increase of the sample during the exposure was determined to be around 1 K. It should be noted that a similar independence of exposure temperatures between 21 and 37 °C could be observed for the induction of structural chromosome aberrations in human lymphocytes by ionizing radiation [Gumrich et al., 1986; Schmid et al., 2003]. Since, however, a steep increase in the aberration yields was found at temperatures varying from 10 to 20 °C, it was concluded that the temperature influences the formation of chromatin lesions, rather than their interaction [Gumrich et al., 1986].

In conclusion, spindle disturbances were found in proliferating human-hamster hybrid FC2 cells which were exposed to EMF at 835 MHz. Therefore, it may be possible that EMF induces biological effects in FC2 cells via non-thermal pathways. However, this result does not necessarily mean that the EMF-induced effects lead to disease or injury, but it is potentially important information for evaluating the underlying mechanisms. Based on the present observations three important questions need to be addressed in the future: (i) Is there any different influence of the electric and the magnetic component of the EMF in question on the biological endpoint in FC2 cells, (ii) what are the underlying mechanism(s) of the induction of such spindle disturbances, and (iii) what is the implication of the present findings to EMF risk assessment? More data are needed from tests in FC2 cells or primary human cells to determine the potency of EMF as a weak or potent aneugen. For example, the presence of a single copy of human chromosome 11 in the FC2 cell line allows the fast automated scoring of fluorescence signals directly on microscopic slides. Applying laser-scanning cytometry as a powerful analysis of the potential of an aneugenic agent [Baumgartner et al., 2001], more insight into the underlying mechanism should be reliably obtained. Additionally, since the human chromosome 11 encodes cell surface antigens (*CD59*) that render FC2 cells sensitive to killing by specific monoclonal antibody E7.1 in the presence of complement, for example, rabbit serum complement, it is also possible to examine any mutagenic potency.

ACKNOWLEDGMENTS

The authors would like to thank Prof. Hermann Weingärtner from the Department Physical Chemistry II, Ruhr—University Bochum, Germany, for the measurement of the complex dielectric properties of the RPMI-1640 medium used.

REFERENCES

Adler ID, Zouh R, Schmid E. 1993. Perturbation of cell division by acrylamide in vitro and in vivo. Mutat Res 301:249–254.

Baumgartner A, Schmid TE, Maerz HK, Adler ID, Tarnok A, Nuesse M. 2001. Automated evaluation of frequencies of aneuploid sperm by laser-scanning cytometry (LSC). Cytometry 44:156–160.

Brusick D, Albertini R, McRee D, Peterson D, Williams G, Hanawalt PJ, Preston J. 1998. Genotoxity of radiofrequency radiation. Environ Mol Mutagen 32:1–16.

Burkhardt M, Pokovic K, Gnos M, Schmid T, Kuster N. 1996. Numerical and experimental dosimetry of Petri dish exposure setups. Bioelectromagnetics 17:483–493.

Compton DA. 2000. Spindle assembly in animal cells. Ann Rev Biochem 69:95–114.

Courant R, Friedrichs K, Lewy H. 1928. On the partial differential equations in mathematical physics (in German). Math Ann 100:32–74.

Crawford ML. 1974. Generation of standard EM fields using TEM transmission cells. IEEE Trans EMC EMC-16:189–195.

CST. 2007. Microwave Studio, Web site http://www.CST.de.

Duesberg P, Slindl R, Hehlmann R. 2000. Explaining the high mutation rates of cancer cells in drug and multidrug resistance by chromosome reassortment that are catalysed by aneuploidy. Proc Natl Acad Sci USA 97:14295–14300.

Glimm J, Münter K, Pape R, Schrader T, Spitzer M. 1997. The New National Standard of EM Field Strength; Realisation and Dissemination; Proc 12th Int Symp on EMC, Zürich, Schweiz, pp 611–613, ISBN 3-9521199-1-1.

GUM-Guideline. 1998. GUM-Guideline: BIPM, IEC; IFCC, ISO, IUPAC, IUPAP, OIML. 1998. Guide to the Expression of Uncertainty in Measurement, 1. Edition, corrected and reprinted, Genf, CH.

Gumrich K, Virsik-Peuckert RP, Harder D. 1986. Temperature and the formation of radiation-induced chromosome aberrations. I. The effect of radiation temperature. Int J Radiat Biol 49: 665–672.

ICNIRP Guidelines. 1998. Guidelines for limiting exposure to time varying electric, magnetic, and electromagnetic fields (up to 300 GHz). Health Phys 74:494–522.

Inoue S, Salmon ED. 1995. Force generation by microtubule assembly/disassembly in mitosis and related movements. Mol Biol Cell 6:1619–1640.

Kazmier LJ, Pohl NF. 1987. Basic statistics for business and economics. New York, NY: McGraw-Hill Co. p. 592.

Kuster N, Schönborn F. 2000. Recommended minimal requirements and development guidelines for exposure setups of bio-experiments addressing the health risk concern of wireless communications. Bioelectromagnetics 21:508–514.

Marklein R. 2002. The finite integration technique as a general tool to compute acoustic, electromagnetic, elastodynamic, and coupled wave fields. In: Stone WR, editor. Review of Radio Science: 1999-2002 URSI. Piscataway and New York: IEEE Press and John Wiley and Sons. pp 201–244.

Mashevich M, Folkman D, Kesar A, Barbul A, Korenstein R, Jerbi E, Avivi L. 2003. Exposure of human peripheral blood lymphocytes to electromagnetic fields associated with cellular phones leads to chromosomal instability. Bioelectromagnetics 24:82–90.

Moulder JE, Erdreich LS, Malyapa RS, Merritt J, Pickard WF, Vijayalaxmi. 1999. Cell phones and cancer: What is the evidence for a connection? Radiat Res 151:513–531.

Moulder JE, Foster KR, Erdreich LS, McNamee JP. 2005. Mobile phones, mobile phone base stations and cancer: A review. Int J Radiat Biol 81:189–203.

Münter K, Pape R, Glimm J. 1997. Portable E-Field strength meter system and its traceable calibration up to 1 GHz using a μTEM cell. IEEE Trans Instr Meas IM-46:549–550.

Nikoloski N, Fröhlich J, Samaras T, Schuderer J, Kuster N. 2005. Reevaluation and improved design of the TEM cell in vitro exposure unit for replication studies. Bioelectromagnetics 26:215–224.

Oshimura M, Barrett JC. 1986. Chemically induced aneuploidy in mammalian cells: Mechanisms and biological significance in cancer. Environ Mutagenesis 8:129–159.

Parry EM, Henderson L, Parry JM. 1995. Procedures for the detection of chemically induced aneuploidy: Recommendations of a UK Environmental Mutagen Society working group. Mutagenesis 10:1–14.

Popovic M, Hagness SC, Taflove A. 1998. Finite-differences time-domain analysis of a complete transverse electromagnetic cell loaded with liquid biological media in culture dishes. IEEE Trans Biomed Eng 45:1067–1076.

Prabhakara K, Murthy AK. 1995. Hyperthermic induction of premature chromosome condensation in human lymphocytes. Mutat Res 331:175–180.

REFLEX. 2004. Risk evaluation of potential environmental hazards from low energy electromagnetic field exposure using sensitive in vitro methods. Final Report http://www.venum-foundation.de.

Sax K. 1937. Effects of variation in temperature on nuclei cell division in tradescantia. Am J Bot 24:218–225.

Scarfi MR, Fresegna AM, Villani P, Pinto R, Marino C, Sarti M, Altavista P, Sannino A, Lovisolo GA. 2006. Exposure to radiofrequency radiation (900 MHz, GSM signal) does not affect micronucleus frequency and cell proliferation in human peripheral blood lymphocytes. An interlaboratory study. Radiat Res 165:655–663.

Schmid E, Bauchinger M. 1976. The cytogenetic effect of an X-ray contrast medium in Chinese hamster cell cultures. Mutat Res 34:291–298.

Schmid E, Schrader T. 2007. Different biological effectiveness of ionising and non-ionising radiations in mammalian cells. Adv Radio Sci 5:1–4.

Schmid E, Schlegel D, Guldbakke S, Kapsch PR, Regulla D. 2003. RBE of nearly monoenergetic neutrons at energies of 36 keV–14.6 MeV for induction of dicentrics in human lymphocytes. Radiat Environ Biophys 42:87–94.

Schrader T, Steinbach D, Münter K, Spitzer M, Glimm J. 1999. Improved performance of the field strength standard μTEM cell. 26. Int General Assembly. Toronto, Canada: International Union of Radio Science.

Speit G, Schuetz P, Hoffmann H. 2007. Genotoxic effects of exposure to radiofrequency electromagnetic fields (RF-EMF) in cultured mammalian cells are not independently reproducible. Mutat Res 626:42–47.

Stronati L, Testa A, Moquet J, Edwards A, Cordelli E, Villani P, Marino C, Fresegna AM, Appolloni M, Lloyd D. 2006. 935 Mhz cellular phone radiation. An in vitro study of genotoxicity in human lymphocytes. Int J Radiat Biol 82:339–346.

Sun FY, Schmid TE, Schmid E, Baumgartner A, Adler ID. 2000. Trichlorfon induces spindle disturbances in V79 cells and aneuploidy in male mouse germ cells. Mutagenesis 15:17–24.

Tice RR, Hook GG, Donner M, McRee DI, Guy AW. 2002. Genotoxicity of radiofrequency signals. I. Investigation of

DNA damage and micronuclei induction in cultured human blood cells. Bioelectromagnetics 23:113–126.

Verschaeve L, Maes A. 1998. Genetic, carcinogenic and teratogenic effects of radiofrequency fields. Mutat Res 410:141–165.

Vig BK, editor. 1993. Chromosome segregation and aneuploidy. NATO ASI Series H72. Berlin, Germany: Springer-Verlag. p. 426.

Vijayalaxmi. 2006. Cytogenetic studies in human blood lymphocytes exposed in vitro to 2.45 GHz or 8.2 GHz radiofrequency radiation. Radiat Res 166:532–538.

Vijayalaxmi, Obe G. 2004. Controversial cytogenetic observations in mammalian somatic cells exposed to radiofrequency radiation. Radiat Res 162:481–496.

Weiland T. 1977. A Discretization Method for the Solution of Maxwell's Equations for Six-Component Fields. Electron Commun (AEÜ) 31:116–120. (see http://www.tu-darmstadt.de/fb/et/temf/).

Yee S. 1966. Numerical solution of initial boundary value problems involving Maxwell's equations in isotropic media. IEEE Trans Antennas Propagation AP-14:302–307.